

Non incremental PGD solution of parametric uncoupled models defined in evolving domains

Amine Ammar¹, Elías Cueto^{2,*}, Francisco Chinesta³

¹ *Arts et Métiers ParisTech*

2 Boulevard du Ronceray, BP 93525, F-49035 Angers cedex 01, France

² *Aragón Institute of Engineering Research (I3A). Universidad de Zaragoza. Edificio Betancourt. María de Luna, s.n. 50018 Zaragoza, Spain.*

³ *EADS Corporate Foundation International Chair. École Centrale de Nantes. 1, Rue de la Noë. 44300 Nantes, France.*

SUMMARY

This work addresses the recurrent issue related to the existence of reduced bases related to the solution of parametric models defined in evolving domains. In this first part of the work we address the case of decoupled kinematics, i.e., models whose solution does not affect the domain in which they are defined. The chosen framework considers an updated Lagrangian description of the kinematics, solved by using natural neighbor Galerkin methods within a non-incremental space-time framework that can be generalized for addressing parametric models. Examples are included showing the performance and potentialities of the proposed methodology.

Copyright © 2010 John Wiley & Sons, Ltd.

KEY WORDS: Model reduction; Proper Generalized Decomposition; Large geometrical transformations; Meshless methods; Natural Element Method; Parametric models.

Contents

1	Introduction	2
1.1	On the difficulty of simulating evolving domains	2
1.2	Reduced order modeling of parametric models: the case of fixed domains	3
1.2.1	Computing $R(\mathbf{x})$ from $S(t)$ and $W(k)$:	4
1.2.2	Computing $S(t)$ from $R(\mathbf{x})$ and $W(k)$:	6
1.2.3	Computing $W(k)$ from $R(\mathbf{x})$ and $S(t)$:	6

*Correspondence to: Elías Cueto. Aragon Institute of Engineering Research. Betancourt Building. Maria de Luna, s.n. 50018 Zaragoza, Spain. e-mail: ecueto@unizar.es

Contract/grant sponsor: Spanish Ministry of Economy and Innovation; contract/grant number: CICYT-DPI2011-27778-C02-01.

2	Separated representation of models defined in evolving domains	7
2.1	Diffusive term	8
2.2	Advective term	9
2.3	Source term	11
3	Building-up the separated representation of the model solution	12
3.1	Computing the space function \mathbf{R}	13
3.2	Computing the time function $\Upsilon(t)$	14
4	Numerical test	14
5	Towards parametric modeling in evolving domains	15
6	Numerical test involving parametric modeling	18
7	conclusions	19

1. Introduction

1.1. On the difficulty of simulating evolving domains

Evolving domains introduce many numerical difficulties. Firstly, when using a fixed mesh the domain evolution must be captured by using an appropriate technique (e.g. VOF, level sets, or any similar technique). The resulting advection terms must be efficiently stabilized by using, in turn, an adequate technique (SUPG, DG, ...). Numerous works have addressed such questions during the last decades see, for instance, [8] and references therein.

Another possibility consists in tracking the domain whose geometry evolves with the material velocity, in an (updated) Lagrangian approach. This approach simplifies the treatment of advection terms that now result in a simple material derivative. The main drawback is, however, that meshes become rapidly too distorted implying the need for frequent remeshing and the associated field projection between old and new meshes. A particularly elegant analysis of the difficulties associated with this approach to the problem can be found in [15]. Intermediate procedures have been proposed in the framework of ALE methods alleviating partially the issues of fixed and moving meshes [8]. However, the determination of the optimal velocity of the mesh is a tricky problem.

Some years ago new discretization techniques were proposed whose accuracy proved to be independent of the nodal distribution used to approximate the different fields involved in the models. These techniques were called meshless or meshfree methods, even if some of them employ a background mesh to construct the functional approximation or even to perform numerical integration. This designation is justified by the fact that the approximation accuracy does not depend on the relative position of the nodes. As a result, remeshing can be avoided even in the case of large distortions of the background mesh.

Despite the chosen framework for the description of the kinematics, it is well known in the reduced order modeling community, that the determination of an efficient set of reduced basis for problems defined in an evolving domain is a difficult task. This is caused, no doubt, because the deformation of the domain very much complicates the concept of *snapshot*, which is crucial

in understanding the overall behavior of the system, and in determining the set of reduced basis itself [20].

In this work, among many different possibilities, we have chosen the Natural Element Method (NEM), widely described in [7] and references therein, to approximate the kinematics in an updated Lagrangian framework. NEM overcomes FEM remeshing needs by employing natural neighbor approximation instead of piece-wise polynomials to construct shape functions in a Galerkin setting. Thus, within the NEM framework one can proceed with the original cloud of nodes moving according to material velocity during the whole simulation, even in the case of very large geometrical transformations. This is not a crucial choice in the development that follows (many other meshless methods exist that allow for an updated Lagrangian description of kinematics), albeit NEM presents some very interesting characteristics that will be analyzed below [1].

In what follows we consider a model defined in a domain that at time $t = 0$ occupies the region $\Omega^0 \subset \mathbb{R}^3$. The different fields in this domain are approximated from a cloud of N_n nodes located at positions $\tilde{\mathbf{x}}_i^0$, $i = 1, \dots, N_n$. The material domain evolves in time, $\Omega(t)$ representing its configuration at time t . We assume that this evolution is defined by a given, decoupled, velocity field $\mathbf{v}(\mathbf{x} \in \Omega(t), t \in \mathcal{I} \subset \mathbb{R}_+)$. Nodes move with the material velocity, and because the meshless behavior of the NEM approximation, all the fields are approximated in the updated domain $\Omega(t)$ by using the original cloud of nodes. No addition or deletion of nodes is considered, even if it is perfectly possible in a NEM framework. At time t nodal positions will be noted by $\tilde{\mathbf{x}}_i^t$, $i = 1, \dots, N_n$.

Hereafter we assume, without loss of generality, that the model, defined in the evolving domain $\Omega(t)$, involves the unknown field $u(\mathbf{x} \in \Omega(t), t \in \mathcal{I})$. We focus on the possibility of determining a reduced basis approximation for such field in the context of the proper generalized decomposition (PGD) framework [3] [14] [5] [6][2][18] [9]. In this work a strategy able to compute transient solutions in evolving domains is proposed. This strategy falls within a non-incremental framework originally proposed in a different context by Ladeveze [13]. Moreover, it will be shown how efficiently parametric models defined in evolving domains can be solved. Here, the model parameter, say the thermal conductivity k of the thermal model here addressed, could be introduced as an extra-coordinate in the model, and then a multidimensional representation of the unknown field $u(\mathbf{x} \in \Omega(t), t \in \mathcal{I}, k \in \mathfrak{S})$ will be found.

1.2. Reduced order modeling of parametric models: the case of fixed domains

In this section, as an introduction, we summarize the PGD-based model reduction strategy for fixed domains. Let us consider the following parametric heat transfer equation:

$$\frac{\partial u}{\partial t} - k\Delta u - s = 0, \quad (1)$$

with homogeneous initial and boundary conditions. Enforcement of non-homogeneous initial and boundary conditions was deeply analyzed in [10].

Here $u = u(\mathbf{x}, t, k) \in \Omega \times I \times \mathfrak{S}$, and the source term s is assumed constant for simplicity. In the PGD framework, the conductivity k is viewed as a new coordinate defined in the interval \mathfrak{S} , rather than as a parameter. Thus, instead of solving the thermal model for different, discrete, values of the conductivity parameter, the strategy developed in [19] and also in [11] aims at solving at once a more general, multidimensional, problem. The price to pay is precisely an increase of the problem dimensionality. However, since the complexity of the PGD

technique scales only linearly (and not exponentially) with the space dimension, considering the conductivity as a new coordinate still allows to efficiently obtain an accurate solution. We review here, precisely, the PGD approach to standard parametric problems.

The weak form related to Eq. (1) reads: *find* $u(\mathbf{x}, t, k)$ *such that*

$$\int_{\Omega \times I \times \mathfrak{S}} u^* \cdot \left(\frac{\partial u}{\partial t} - k \cdot \Delta u - s \right) d\mathbf{x} \cdot dt \cdot dk = 0, \quad (2)$$

for all test functions u^* selected in an appropriate functional space.

The PGD solution is sought iteratively in the form [3]:

$$u(\mathbf{x}, t, k) \approx \sum_{i=1}^N X_i(\mathbf{x}) \cdot T_i(t) \cdot K_i(k). \quad (3)$$

Let us assume that the n -th term of the PGD approximation is already known:

$$u^n(\mathbf{x}, t, k) = \sum_{i=1}^n X_i(\mathbf{x}) \cdot T_i(t) \cdot K_i(k). \quad (4)$$

Computation of the $n + 1$ -th term $X_{n+1}(\mathbf{x}) \cdot T_{n+1}(t) \cdot K_{n+1}(k)$, which we write as $R(\mathbf{x}) \cdot S(t) \cdot W(k)$ for simplicity,

$$u^{n+1} = u^n + R(\mathbf{x}) \cdot S(t) \cdot W(k). \quad (5)$$

begins by assuming the simplest choice for the test functions u^* used in Eq. (2):

$$u^* = R^*(\mathbf{x}) \cdot S(t) \cdot W(k) + R(\mathbf{x}) \cdot S^*(t) \cdot W(k) + R(\mathbf{x}) \cdot S(t) \cdot W^*(k). \quad (6)$$

With the trial and test functions given by Eqs. (5) and (6) respectively, Eq. (2) is a non-linear problem that must be solved by means of a suitable iterative scheme. In our earlier papers [3] and [4], we used Newton's method. Simpler linearization strategies can also be applied, however. The simplest one is an alternating direction, fixed-point algorithm, which was found remarkably robust in the present context. Each iteration consists of three steps that are repeated until convergence, that is, until reaching the fixed point. The first step assumes $S(t)$ and $W(k)$ known from the previous iteration and computes an update for $R(\mathbf{x})$ (in this case the test function reduces to $R^*(\mathbf{x}) \cdot S(t) \cdot W(k)$). From the just updated $R(\mathbf{x})$ and the previously used $W(k)$, we can update $S(t)$ (with $u^* = R(\mathbf{x}) \cdot S^*(t) \cdot W(k)$). Finally, from the just computed $R(\mathbf{x})$ and $S(t)$, we update $W(k)$ (with $u^* = R(\mathbf{x}) \cdot S(t) \cdot W^*(k)$). This iterative procedure continues until reaching convergence. The converged functions $R(\mathbf{x})$, $S(t)$ and $W(k)$ yield the new functional product of the current enrichment step: $X_{n+1}(\mathbf{x}) = R(\mathbf{x})$, $T_{n+1}(t) = S(t)$ and $K_{n+1}(k) = W(k)$. The explicit form of these operations is described below.

1.2.1. Computing $R(\mathbf{x})$ from $S(t)$ and $W(k)$: We consider the weak form of equation (1):

$$\int_{\Omega \times I \times \mathfrak{S}} u^* \cdot \left(\frac{\partial u}{\partial t} - k \cdot \Delta u - s \right) d\mathbf{x} \cdot dt \cdot dk = 0, \quad (7)$$

Here, the trial function is given by

$$u(\mathbf{x}, t, k) = \sum_{i=1}^n X_i(\mathbf{x}) \cdot T_i(t) \cdot K_i(k) + R(\mathbf{x}) \cdot S(t) \cdot W(k). \quad (8)$$

Since S and W are known from the previous iteration, the test function reads

$$u^*(\mathbf{x}, t, k) = R^*(\mathbf{x}) \cdot S(t) \cdot W(k). \quad (9)$$

Introducing (8) and (9) into (7) yields

$$\begin{aligned} \int_{\Omega \times I \times \mathfrak{S}} R^* \cdot S \cdot W \cdot \left(R \cdot \frac{\partial S}{\partial t} \cdot W - k \cdot \Delta R \cdot S \cdot W \right) d\mathbf{x} dt dk = \\ = - \int_{\Omega \times I \times \mathfrak{S}} R^* \cdot S \cdot W \cdot \mathcal{R}^n d\mathbf{x} dt dk, \end{aligned} \quad (10)$$

where \mathcal{R}^n stands for the residual at enrichment step n :

$$\mathcal{R}^n = \sum_{i=1}^n X_i \cdot \frac{\partial T_i}{\partial t} \cdot K_i - \sum_{i=1}^n k \cdot \Delta X_i \cdot T_i \cdot K_i - s. \quad (11)$$

Since all functions depending time and conductivity have been already determined, we can integrate Eq. (10) over $I \times \mathfrak{S}$. With the following notations,

$$\left[\begin{array}{lll} w_1 = \int_{\mathfrak{S}} W^2 dk & s_1 = \int_I S^2 dt & r_1 = \int_{\Omega} R^2 d\mathbf{x} \\ w_2 = \int_{\mathfrak{S}} kW^2 dk & s_2 = \int_I S \cdot \frac{dS}{dt} dt & r_2 = \int_{\Omega} R \cdot \Delta R d\mathbf{x} \\ w_3 = \int_{\mathfrak{S}} W dk & s_3 = \int_I S dt & r_3 = \int_{\Omega} R d\mathbf{x} \\ w_4^i = \int_{\mathfrak{S}} W \cdot K_i dk & s_4^i = \int_I S \cdot \frac{dT_i}{dt} dt & r_4^i = \int_{\Omega} R \cdot \Delta X_i d\mathbf{x} \\ w_5^i = \int_{\mathfrak{S}} kW \cdot K_i dk & s_5^i = \int_I S \cdot T_i dt & r_5^i = \int_{\Omega} R \cdot X_i d\mathbf{x} \end{array} \right], \quad (12)$$

Eq. (10) reduces to

$$\begin{aligned} \int_{\Omega} R^* \cdot (w_1 \cdot s_2 \cdot R - w_2 \cdot s_1 \cdot \Delta R) d\mathbf{x} = \\ = - \int_{\Omega} R^* \cdot \left(\sum_{i=1}^n w_4^i \cdot s_4^i \cdot X_i - \sum_{i=1}^n w_5^i \cdot s_5^i \cdot \Delta X_i - w_3 \cdot s_3 \cdot s \right) d\mathbf{x}. \end{aligned} \quad (13)$$

Eq. (13) defines in weak form an elliptic steady-state boundary value problem for the unknown function R that can be solved by using any suitable discretization technique (finite elements, finite volumes, ...). Another possibility consists in coming back to the strong form of Eq. (13):

$$\begin{aligned} w_1 \cdot s_2 \cdot R - w_2 \cdot s_1 \cdot \Delta R = \\ = - \left(\sum_{i=1}^n w_4^i \cdot s_4^i \cdot X_i - \sum_{i=1}^n w_5^i \cdot s_5^i \cdot \Delta X_i - w_3 \cdot s_3 \cdot s \right), \end{aligned} \quad (14)$$

that can be solved by using any classical collocation technique (finite differences, SPH, ...).

1.2.2. *Computing $S(t)$ from $R(\mathbf{x})$ and $W(k)$:* In the present case, the test function is written as

$$u^*(\mathbf{x}, t, k) = S^*(t) \cdot R(\mathbf{x}) \cdot W(k), \quad (15)$$

and the weak form becomes

$$\begin{aligned} \int_{\Omega \times I \times \mathfrak{S}} S^* \cdot R \cdot W \cdot \left(R \cdot \frac{\partial S}{\partial t} \cdot W - k \cdot \Delta R \cdot S \cdot W \right) d\mathbf{x} dt dk = \\ = - \int_{\Omega \times I \times \mathfrak{S}} S^* \cdot R \cdot W \cdot \mathcal{R}^n d\mathbf{x} dt dk. \end{aligned} \quad (16)$$

Integrating over $\Omega \times \mathfrak{S}$ gives

$$\begin{aligned} \int_I S^* \cdot \left(w_1 \cdot r_1 \cdot \frac{dS}{dt} - w_2 \cdot r_2 \cdot S \right) dt = \\ = - \int_I S^* \cdot \left(\sum_{i=1}^n w_4^i \cdot r_5^i \cdot \frac{dT_i}{dt} - \sum_{i=1}^n w_5^i \cdot r_4^i \cdot T_i - w_3 \cdot r_3 \cdot s \right) dt. \end{aligned} \quad (17)$$

Equation (17) represents the weak form of the ODE defining the time evolution of the field S that can be solved by using any stabilized discretization technique (SU, Discontinuous Galerkin, ...). The strong form of Eq. (17) reads

$$\begin{aligned} w_1 \cdot r_1 \cdot \frac{dS}{dt} - w_2 \cdot r_2 \cdot S = \\ = - \left(\sum_{i=1}^n w_4^i \cdot r_5^i \cdot \frac{dT_i}{dt} - \sum_{i=1}^n w_5^i \cdot r_4^i \cdot T_i - w_3 \cdot r_3 \cdot s \right). \end{aligned} \quad (18)$$

Equation (18) can be solved by using backward finite differences, or higher order Runge-Kutta schemes, among many other possibilities.

1.2.3. *Computing $W(k)$ from $R(\mathbf{x})$ and $S(t)$:* The test function is now given by

$$u^*(\mathbf{x}, t, k) = W^*(k) \cdot R(\mathbf{x}) \cdot S(t), \quad (19)$$

and the weak form becomes

$$\begin{aligned} \int_{\Omega \times I \times \mathfrak{S}} W^* \cdot R \cdot S \cdot \left(R \cdot \frac{\partial S}{\partial t} \cdot W - k \cdot \Delta R \cdot S \cdot W \right) d\mathbf{x} dt dk = \\ = - \int_{\Omega \times I \times \mathfrak{S}} W^* \cdot R \cdot S \cdot \mathcal{R}^n d\mathbf{x} dt dk. \end{aligned} \quad (20)$$

Integration over $\Omega \times I$ yields

$$\begin{aligned} \int_{\mathfrak{S}} W^* \cdot (r_1 \cdot s_2 \cdot W - r_2 \cdot s_1 \cdot k \cdot W) dk = \\ = - \int_{\mathfrak{S}} W^* \cdot \left(\sum_{i=1}^n r_5^i \cdot s_4^i \cdot K_i - \sum_{i=1}^n r_4^i \cdot s_5^i \cdot k \cdot K_i - r_3 \cdot s_3 \cdot s \right) dk. \end{aligned} \quad (21)$$

Equation (21) does not involve any differential operator. The corresponding strong form reads

$$(r_1 \cdot s_2 - r_2 \cdot s_1 \cdot k) \cdot W = - \left(\sum_{i=1}^n (r_5^i \cdot s_4^i - r_4^i \cdot s_5^i \cdot k) \cdot K_i - r_3 \cdot s_3 \cdot s \right). \quad (22)$$

This is actually an algebraic problem, which is hardly a surprise since the original equation (1) does not contain derivatives with respect to the parameter k . Introduction of the parameter k as an additional model coordinate does not increase the cost of a particular enrichment step. It does however necessitate more enrichment steps, i.e. more terms (higher N) in the decomposition (3).

Remark 1. *The just described procedure assumes that Ω does not depend on time in order to decouple the space and time problems.*

Remark 2. *We have seen that at each enrichment step the construction of the new functional product in Eq. (3) requires non-linear iterations. If m_i denotes the number of iterations needed at enrichment step i , the total number of iterations involved in the construction of the PGD approximation is $m = \sum_{i=1}^N m_i$. In the example above, the entire procedure thus involves the solution of m three-dimensional problems for the functions $X_i(\mathbf{x})$, m one-dimensional problems for the functions $T_i(t)$ and m algebraic systems for the functions $K_i(k)$. In general, m rarely exceeds ten. The number N of functional products needed to approximate the solution with enough accuracy depends on the solution regularity. All numerical experiments carried to date reveal that N ranges between a few tens and one hundred. Thus, we can conclude that the complexity of the PGD procedure to compute the approximation (3) is of some tens of 3D steady-state problems (the cost related to the 1D and algebraic problems being negligible with respect to the 3D problems). In a classical approach, one must solve for each particular value of the parameter k a 3D problem at each time step. In usual applications, this often implies the computation of several millions of 3D solutions. Clearly, the CPU time savings by applying the PGD can be of several orders of magnitude.*

2. Separated representation of models defined in evolving domains

In order to show how the just explained strategy can be extended to problems defined in evolving domains, we come back to a non-parametric problem, for the sake of simplicity in the exposition (the procedure below can straightforwardly be extended to parametric problems as in the previous section), and consider the advection diffusion equation defined in a domain $\Omega(t)$ that evolves with a prescribed velocity field $\mathbf{v}(\mathbf{x}, t)$, $\mathbf{x} \in \Omega(t)$ and $t \in \mathcal{I}$. Without loss of generality we assume homogeneous initial and boundary conditions. The issue related to the enforcement of non homogeneous boundary conditions was deeply addressed in [10].

The weak form of the problem, in this case, reads: *find $u(\mathbf{x}, t)$ such that*

$$\int_{\mathcal{I}} \int_{\Omega(t)} u^* \cdot \left(\frac{Du}{Dt} - k \cdot \Delta u - s \right) d\mathbf{x} \cdot dt = 0 \quad (23)$$

holds for every test function u^* defined in an appropriate Hilbert space. The source term is considered depending on the space and time coordinates, i.e. $s(\mathbf{x}, t)$.

By integrating by parts, the weak form writes:

$$\int_{\mathcal{I}} \int_{\Omega(t)} \left(u^* \cdot \frac{Du}{Dt} + k \cdot \nabla u^* \cdot \nabla u - u^* \cdot s \right) d\mathbf{x} \cdot dt = 0 \quad (24)$$

The approximation of the field $u(\mathbf{x}, t)$ is constructed from nodal values $u_i^t \equiv u(\tilde{\mathbf{x}}_i^t, t)$ by utilizing a natural neighbor (NN) interpolation:

$$u(\mathbf{x} \in \Omega(t), t) \approx \sum_{i=1}^{i=N_n} N_i^t(\mathbf{x}) \cdot u_i^t = \mathbf{N}^t \cdot \mathbf{U}^t \quad (25)$$

where the upper-index t associated to the shape functions N_i^t indicates that these shape functions were defined from the nodal positions $\tilde{\mathbf{x}}_i^t$ in $\Omega(t)$.

As mentioned before, although it is by no means the only possible choice, NN interpolation has remarkable properties that make their use in this context very convenient [7]. Undoubtedly, one of them is the Kroenecker delta property that states:

$$N_i^t(\tilde{\mathbf{x}}_j^t) = \delta_{ij} \quad (26)$$

that, together with the exact interpolation on boundaries, makes it possible to easily enforce Dirichlet boundary conditions.

In what follows we analyze separately the different terms in Eq. (24).

2.1. Diffusive term

We consider the diffusive term in Eq. (24):

$$\mathcal{D} = \int_{\mathcal{I}} \int_{\Omega(t)} k \cdot \nabla u^* \cdot \nabla u \, d\mathbf{x} \cdot dt \quad (27)$$

If we define a matrix \mathbf{B}^t containing the derivatives of the shape functions N_i^t :

$$\mathbf{B}^t = \begin{pmatrix} \frac{dN_1^t}{dx} & \frac{dN_2^t}{dx} & \dots & \frac{dN_n^t}{dx} \\ \frac{dN_1^t}{dy} & \frac{dN_2^t}{dy} & \dots & \frac{dN_n^t}{dy} \\ \frac{dN_1^t}{dz} & \frac{dN_2^t}{dz} & \dots & \frac{dN_n^t}{dz} \end{pmatrix} \quad (28)$$

the diffusive term can be written as:

$$\begin{aligned} \mathcal{D} &= \int_{\mathcal{I}} \int_{\Omega(t)} k \cdot \mathbf{U}^{*T} \cdot \mathbf{B}^{tT} \cdot \mathbf{B}^t \cdot \mathbf{U}^t \, d\mathbf{x} \cdot dt = \\ &= \int_{\mathcal{I}} k \cdot \mathbf{U}^{*T} \cdot \left(\int_{\Omega(t)} \mathbf{B}^{tT} \cdot \mathbf{B}^t \, d\mathbf{x} \right) \cdot \mathbf{U}^t \, dt = \int_{\mathcal{I}} k \cdot \mathbf{U}^{*T} \cdot \mathbf{G}(t) \cdot \mathbf{U}^t \, dt \end{aligned} \quad (29)$$

Because $\Omega(t)$ is known $\forall t$, we can evaluate the integral

$$\mathbf{G}_k = \int_{\Omega(t_k)} \mathbf{B}^{t_k T} \cdot \mathbf{B}^{t_k} \, d\mathbf{x} \quad (30)$$

at different times t_k , $k = 1, \dots, Q$.

Following the spirit of Karhunen-Loeve transform or proper orthogonal decompositions, see [12] [16] [17], from these integrals we could define a matrix \mathbf{G}

$$\mathbf{G} = (\mathbf{G}_1 \mathbf{G}_2 \cdots \mathbf{G}_Q) \quad (31)$$

that, after applying a singular value decomposition (SVD), gives

$$\mathbf{G}(t) = \int_{\Omega(t)} \mathbf{B}^{t^T} \cdot \mathbf{B}^t \, d\mathbf{x} \approx \sum_{j=1}^{j=m_1} F_j^d(t) \cdot \mathbf{E}_j^d \quad (32)$$

with $m_1 < Q$ and $m_1 < N_n$.

Thus, the diffusive term can be advantageously written as :

$$\begin{aligned} \mathcal{D} &= \int_{\mathcal{I}} \int_{\Omega(t)} k \cdot \mathbf{U}^{*^T} \cdot \mathbf{B}^{t^T} \cdot \mathbf{B}^t \cdot \mathbf{U}^t \, d\mathbf{x} \cdot dt = \\ &= \int_{\mathcal{I}} k \cdot \mathbf{U}^{*^T} \cdot \left(\sum_{j=1}^{j=m_1} F_j^d(t) \cdot \mathbf{E}_j^d \right) \cdot \mathbf{U}^t \, dt \quad (33) \end{aligned}$$

2.2. Advective term

We consider now the term involving time derivatives:

$$\mathcal{A} = \int_{\mathcal{I}} \int_{\Omega(t)} u^* \cdot \frac{Du}{Dt} \, d\mathbf{x} \cdot dt. \quad (34)$$

The material derivative $\frac{Du}{Dt}$ writes when using a fixed reference system

$$\frac{Du}{Dt} = \frac{\partial u}{\partial t} + \mathbf{v} \cdot \nabla u. \quad (35)$$

However, when the reference system follows matter, the advective term can be discretized along the characteristic lines according to:

$$\frac{Du}{Dt} \approx \frac{u(\mathbf{x}, t) - \hat{u}(\mathbf{x}, t)}{\Delta t} \quad (36)$$

where

$$\hat{u}(\mathbf{x}, t) = u(\mathbf{x} - \mathbf{v} \cdot \Delta t, t - \Delta t) \quad (37)$$

represents the root of the characteristic line at the previous time step, and hence the advantages of using an updated Lagrangian frame of reference.

Thus, if the time interval \mathcal{I} is decomposed in P time steps of length Δt , i.e. $\mathcal{I} = [0, P \cdot \Delta t]$, Eq. (34) reduces to:

$$\mathcal{A} \approx \sum_{p=1}^{p=P} \int_{\Omega(t_p)} u^* \cdot (u(\mathbf{x}, t_p) - \hat{u}(\mathbf{x}, t_p)) \, d\mathbf{x} \quad (38)$$

that is composed of two terms:

$$\mathcal{A}_1 \approx \sum_{p=1}^{p=P} \int_{\Omega(t_p)} u^* \cdot u(\mathbf{x}, t_p) \, d\mathbf{x} \quad (39)$$

and

$$\mathcal{A}_2 \approx \sum_{p=1}^{p=P} \int_{\Omega(t_p)} u^* \cdot \hat{u}(\mathbf{x}, t_p) d\mathbf{x} \quad (40)$$

Considering the approximation given by Eq. (25) it results

$$\mathcal{A}_1 \approx \sum_{p=1}^{p=P} \mathbf{U}^{*T} \cdot \left(\int_{\Omega(t_p)} \mathbf{N}^{t_p T} \cdot \mathbf{N}^{t_p} d\mathbf{x} \right) \cdot \mathbf{U}^{t_p} = \sum_{p=1}^{p=P} \mathbf{U}^{*T} \cdot \mathbf{M}(t_p) \cdot \mathbf{U}^{t_p} \quad (41)$$

Since $\Omega(t)$ is known $\forall t$, we can easily evaluate the integral

$$\mathbf{M}_k = \int_{\Omega(t_k)} \mathbf{N}^{t_k T} \cdot \mathbf{N}^{t_k} d\mathbf{x} \quad (42)$$

at different times t_k , $k = 1, \dots, Q$.

Again, from these integrals we can define a matrix \mathbf{M}

$$\mathbf{M} = (\mathbf{M}_1 \mathbf{M}_2 \dots \mathbf{M}_Q) \quad (43)$$

that after applying a singular value decomposition (SVD) allows writing

$$\mathbf{M}(t) = \int_{\Omega(t)} \mathbf{N}^{t T} \cdot \mathbf{N}^t d\mathbf{x} \approx \sum_{j=1}^{j=m_2} F_j^a(t) \cdot \mathbf{E}_j^a \quad (44)$$

with $m_2 < Q$ and $m_2 < N_n$.

Thus, the term \mathcal{A}_1 reads:

$$\mathcal{A}_1 \approx \sum_{p=1}^{p=P} \mathbf{U}^{*T} \cdot \left(\sum_{j=1}^{j=m_2} F_j^a(t_p) \cdot \mathbf{E}_j^a \right) \cdot \mathbf{U}^{t_p} \quad (45)$$

Now, we come back to the second contribution \mathcal{A}_2 . Firstly we define the approximation of $\hat{u}(\mathbf{x}, t)$:

$$\hat{u}(\mathbf{x} \in \Omega(t), t) \approx \sum_{i=1}^{i=N_n} \hat{N}_i(\mathbf{x}) \cdot u_i^{t-\Delta t} = \hat{\mathbf{N}} \cdot \mathbf{U}^{t-\Delta t} \quad (46)$$

from which the integral \mathcal{A}_2 now reads

$$\mathcal{A}_2 \approx \sum_{p=1}^{p=P} \mathbf{U}^{*T} \cdot \left(\int_{\Omega(t_p)} \mathbf{N}^{t_p T} \cdot \hat{\mathbf{N}} d\mathbf{x} \right) \cdot \mathbf{U}^{t_p-\Delta t} = \sum_{p=1}^{p=P} \mathbf{U}^{*T} \cdot \hat{\mathbf{M}}(t_p) \cdot \mathbf{U}^{t_p-\Delta t} \quad (47)$$

Because $\Omega(t)$ is known $\forall t$, we can evaluate the integral

$$\hat{\mathbf{M}}_k = \int_{\Omega(t_k)} \mathbf{N}^{t_k T} \cdot \hat{\mathbf{N}} d\mathbf{x} \quad (48)$$

at different times t_k , $k = 1, \dots, Q$.

From these integrals we could define a matrix $\hat{\mathbf{M}}$

$$\hat{\mathbf{M}} = (\hat{\mathbf{M}}_1, \hat{\mathbf{M}}_2, \dots, \hat{\mathbf{M}}_Q) \quad (49)$$

that by applying a singular value decomposition (SVD) allows writing

$$\hat{\mathbf{M}}(t) = \int_{\Omega(t)} \mathbf{N}^{t^T} \cdot \hat{\mathbf{N}} \, d\mathbf{x} \approx \sum_{j=1}^{j=m_3} F_j^u(t) \cdot \mathbf{E}_j^u \quad (50)$$

with $m_3 < Q$ and $m_3 < N_n$.

Thus, the term \mathcal{A}_2 reads:

$$\mathcal{A}_2 \approx \sum_{p=1}^{p=P} \mathbf{U}^{*^T} \cdot \left(\sum_{j=1}^{j=m_3} F_j^u(t_p) \cdot \mathbf{E}_j^u \right) \cdot \mathbf{U}^{t_p - \Delta t} \quad (51)$$

2.3. Source term

We consider the source term in Eq. (24):

$$\mathcal{S} = \int_{\mathcal{I}} \int_{\Omega(t)} u^* \cdot s(\mathbf{x}, t) \, d\mathbf{x} \cdot dt \quad (52)$$

By approximating the source term from:

$$s(\mathbf{x} \in \Omega(t), t) \approx \sum_{i=1}^{i=N_n} N_i^t(\mathbf{x}) \cdot s_i^t = \mathbf{N}^t \cdot \mathbf{S}^t \quad (53)$$

the source term in the weak form of the problem can be written as:

$$\begin{aligned} \mathcal{S} &= \int_{\mathcal{I}} \int_{\Omega(t)} \mathbf{U}^{*^T} \cdot \mathbf{N}^{t^T} \cdot \mathbf{N}^t \cdot \mathbf{S}^t \, d\mathbf{x} \cdot dt = \\ &= \int_{\mathcal{I}} \mathbf{U}^{*^T} \cdot \left(\int_{\Omega(t)} \mathbf{N}^{t^T} \cdot \mathbf{N}^t \, d\mathbf{x} \right) \cdot \mathbf{S}^t \, dt = \int_{\mathcal{I}} \mathbf{U}^{*^T} \cdot \mathbf{M}(t) \cdot \mathbf{S}^t \, dt \end{aligned} \quad (54)$$

which, considering the previous developments, results in:

$$\begin{aligned} \mathcal{S} &= \int_{\mathcal{I}} \int_{\Omega(t)} \mathbf{U}^{*^T} \cdot \mathbf{N}^{t^T} \cdot \mathbf{N}^t \cdot \mathbf{S}^t \, d\mathbf{x} \cdot dt = \\ &= \int_{\mathcal{I}} \mathbf{U}^{*^T} \cdot \left(\sum_{j=1}^{j=m_2} F_j^a(t) \cdot \mathbf{E}_j^a \right) \cdot \mathbf{S}^t \, dt \end{aligned} \quad (55)$$

By applying again a singular value decomposition \mathbf{S}^t can be expressed in a separated form:

$$\mathbf{S}^t \approx \sum_{l=1}^{l=L} C_l(t) \cdot \mathbf{D}_l \quad (56)$$

leading to:

$$\mathcal{S} = \int_{\mathcal{I}} \mathbf{U}^{*^T} \cdot \left(\sum_{j=1}^{j=m_2} F_j^a(t) \cdot \mathbf{E}_j^a \right) \cdot \left(\sum_{l=1}^{l=L} C_l(t) \cdot \mathbf{D}_l \right) \, dt \quad (57)$$

3. Building-up the separated representation of the model solution

Once the problem has been stated in a separated form, by applying SVD to every term in its weak form, the technique here proposed proceeds by constructing a separated, space-time, representation for the solution, $u = u(\mathbf{x}, t)$. In the mentioned separated representation, the model reads:

$$\begin{aligned} \sum_{p=1}^{k=P} \mathbf{U}^{*T} \cdot \left(\sum_{j=1}^{j=m_2} F_j^a(t_p) \cdot \mathbf{E}_j^a \right) \cdot \mathbf{U}^{t_p} - \\ - \sum_{p=1}^{p=P} \mathbf{U}^{*T} \cdot \left(\sum_{j=1}^{j=m_3} F_j^u(t_p) \cdot \mathbf{E}_j^u \right) \cdot \mathbf{U}^{t_p - \Delta t} + \\ + \int_{\mathcal{I}} k \cdot \mathbf{U}^{*T} \cdot \left(\sum_{j=1}^{j=m_1} F_j^d(t) \cdot \mathbf{E}_j^d \right) \cdot \mathbf{U}^t dt - \\ - \int_{\mathcal{I}} \mathbf{U}^{*T} \cdot \left(\sum_{j=1}^{j=m_2} F_j^a(t) \cdot \mathbf{E}_j^a \right) \cdot \mathbf{S}^t dt = 0 \quad (58) \end{aligned}$$

Assuming that the model solution accepts a separated space-time representation, one could look for an a priori separated representation of \mathbf{U}^t :

$$\mathbf{U}^t \approx \sum_{i=1}^{i=N} T_i(t) \cdot \mathbf{X}_i \quad (59)$$

For constructing such an approximation we proceed by computing a term of the finite sum at each iteration. Thus, we assume at iteration n that the n first terms of the sum have been already calculated, from which we can write the n -th order approximation of \mathbf{U}^t

$$\mathbf{U}^t \approx \sum_{i=1}^{i=n} T_i(t) \cdot \mathbf{X}_i \quad (60)$$

At the following iteration, $n+1$, we are looking for the new functional product $T_{n+1}(t) \cdot \mathbf{X}_{n+1}$. For the sake of simplicity functions $T_{n+1}(t)$ and \mathbf{X}_{n+1} will be noted by Υ and \mathbf{R} respectively, where the dependence on t of Υ is omitted for the sake of clarity.

Thus, the $(n+1)$ -th order approximation reads:

$$\mathbf{U}^t \approx \sum_{i=1}^{i=n} T_i(t) \cdot \mathbf{X}_i + \Upsilon \cdot \mathbf{R} \quad (61)$$

To compute both functions Υ and \mathbf{R} we consider Eq. (58), where the trial function is given by (61) and the test function by:

$$\mathbf{U}^* = \Upsilon^* \cdot \mathbf{R} + \Upsilon \cdot \mathbf{R}^* \quad (62)$$

Since the resulting problem is non-linear, because of the product of both unknown functions Υ and \mathbf{R} , a linearization is therefore compulsory. The simplest one consists, as explained

before, of a fixed point, alternating directions, strategy that computes \mathbf{R} by assuming known Υ , then Υ from the just updated \mathbf{R} . Both steps are repeated until reaching the fixed point of both Υ and \mathbf{R} .

In what follows we are detailing both steps.

3.1. Computing the space function \mathbf{R}

When Υ is assumed known, the test function \mathbf{U}^* reduces to $\mathbf{U}^* = \Upsilon \cdot \mathbf{R}^*$. In this case the integral form writes:

$$\begin{aligned} & \sum_{p=1}^{p=P} \mathbf{R}^{*T} \cdot \Upsilon(t_p) \cdot \left(\sum_{j=1}^{j=m_2} F_j^a(t_p) \cdot \mathbf{E}_j^a \right) \cdot \left(\sum_{i=1}^{i=n} T_i(t_p) \cdot \mathbf{X}_i + \Upsilon(t_p) \cdot \mathbf{R} \right) - \\ & - \sum_{p=1}^{p=P} \mathbf{R}^{*T} \cdot \Upsilon(t_p) \cdot \left(\sum_{j=1}^{j=m_3} F_j^u(t_p) \cdot \mathbf{E}_j^u \right) \cdot \left(\sum_{i=1}^{i=n} T_i(t_{p-1}) \cdot \mathbf{X}_i + \Upsilon(t_{p-1}) \cdot \mathbf{R} \right) + \\ & + \int_{\mathcal{I}} \mathbf{R}^{*T} \cdot k \cdot \Upsilon(t) \cdot \left(\sum_{j=1}^{j=m_1} F_j^d(t) \cdot \mathbf{E}_j^d \right) \cdot \left(\sum_{i=1}^{i=n} T_i(t) \cdot \mathbf{X}_i + \Upsilon(t) \cdot \mathbf{R} \right) dt - \\ & - \int_{\mathcal{I}} \mathbf{R}^{*T} \cdot \Upsilon(t) \cdot \left(\sum_{j=1}^{j=m_2} F_j^a(t) \cdot \mathbf{E}_j^a \right) \cdot \left(\sum_{l=1}^{l=L} C_l(t) \cdot \mathbf{D}_l \right) dt = 0 \quad (63) \end{aligned}$$

where $t_{p-1} = t_p - \Delta t$.

By using a simple numerical quadrature, the previous equation becomes:

$$\begin{aligned} & \sum_{p=1}^{p=P} \mathbf{R}^{*T} \cdot \Upsilon(t_p) \cdot \left(\sum_{j=1}^{j=m_2} F_j^a(t_p) \cdot \mathbf{E}_j^a \right) \cdot \left(\sum_{i=1}^{i=n} T_i(t_p) \cdot \mathbf{X}_i + \Upsilon(t_p) \cdot \mathbf{R} \right) - \\ & - \sum_{p=1}^{p=P} \mathbf{R}^{*T} \cdot \Upsilon(t_p) \cdot \left(\sum_{j=1}^{j=m_3} F_j^u(t_p) \cdot \mathbf{E}_j^u \right) \cdot \left(\sum_{i=1}^{i=n} T_i(t_{p-1}) \cdot \mathbf{X}_i + \Upsilon(t_{p-1}) \cdot \mathbf{R} \right) + \\ & + \sum_{p=1}^{p=P} \mathbf{R}^{*T} \cdot k \cdot \Upsilon(t_p) \cdot \left(\sum_{j=1}^{j=m_1} F_j^d(t_p) \cdot \mathbf{E}_j^d \right) \cdot \left(\sum_{i=1}^{i=n} T_i(t_p) \cdot \mathbf{X}_i + \Upsilon(t_p) \cdot \mathbf{R} \right) \cdot \Delta t - \\ & - \sum_{p=1}^{p=P} \mathbf{R}^{*T} \cdot \Upsilon(t_p) \cdot \left(\sum_{j=1}^{j=m_2} F_j^a(t_p) \cdot \mathbf{E}_j^a \right) \cdot \left(\sum_{l=1}^{l=L} C_l(t_p) \cdot \mathbf{D}_l \right) \cdot \Delta t = 0 \quad (64) \end{aligned}$$

Because of the arbitrariness of \mathbf{R}^* , after developing all the calculations, Eq. (64) results in a linear system:

$$\mathbf{H} \cdot \mathbf{R} = \mathbf{Z} \quad (65)$$

from which we can update vector \mathbf{R} .

3.2. Computing the time function $\Upsilon(t)$

When \mathbf{R} is assumed known, the test function \mathbf{U}^* reduces to $\mathbf{U}^* = \Upsilon^* \cdot \mathbf{R}$. In this case is easy to verify that the discrete form reads:

$$\begin{aligned} & \sum_{p=1}^{p=P} \Upsilon^*(t_p) \cdot \mathbf{R}^T \cdot \left(\sum_{j=1}^{j=m_2} F_j^a(t_p) \cdot \mathbf{E}_j^a \right) \cdot \left(\sum_{i=1}^{i=n} T_i(t_p) \cdot \mathbf{X}_i + \Upsilon(t_p) \cdot \mathbf{R} \right) - \\ & - \sum_{p=1}^{p=P} \Upsilon^*(t_p) \cdot \mathbf{R}^T \cdot \left(\sum_{j=1}^{j=m_3} F_j^u(t_p) \cdot \mathbf{E}_j^u \right) \cdot \left(\sum_{i=1}^{i=n} T_i(t_{p-1}) \cdot \mathbf{X}_i + \Upsilon(t_{p-1}) \cdot \mathbf{R} \right) + \\ & + \sum_{p=1}^{p=P} \Upsilon^*(t_p) \cdot \mathbf{R}^T \cdot k \cdot \left(\sum_{j=1}^{j=m_1} F_j^d(t_p) \cdot \mathbf{E}_j^d \right) \cdot \left(\sum_{i=1}^{i=n} T_i(t_p) \cdot \mathbf{X}_i + \Upsilon(t_p) \cdot \mathbf{R} \right) \cdot \Delta t - \\ & - \sum_{p=1}^{p=P} \Upsilon^*(t_p) \cdot \mathbf{R}^T \cdot \left(\sum_{j=1}^{j=m_2} F_j^a(t_p) \cdot \mathbf{E}_j^a \right) \cdot \left(\sum_{l=1}^{l=L} C_l(t_p) \cdot \mathbf{D}_l \right) \cdot \Delta t = 0 \quad (66) \end{aligned}$$

Since we are assuming homogeneous initial condition, this results in $\Upsilon(t_0) = 0$.

Then, the arbitrariness of $\Upsilon^*(t_p)$, $\forall p \geq 1$ implies:

$$\begin{aligned} & \mathbf{R}^T \cdot \left(\sum_{j=1}^{j=m_2} F_j^a(t_p) \cdot \mathbf{E}_j^a \right) \cdot \left(\sum_{i=1}^{i=n} T_i(t_p) \cdot \mathbf{X}_i + \Upsilon(t_p) \cdot \mathbf{R} \right) - \\ & - \mathbf{R}^T \cdot \left(\sum_{j=1}^{j=m_3} F_j^u(t_p) \cdot \mathbf{E}_j^u \right) \cdot \left(\sum_{i=1}^{i=n} T_i(t_{p-1}) \cdot \mathbf{X}_i + \Upsilon(t_{p-1}) \cdot \mathbf{R} \right) + \\ & + \mathbf{R}^T \cdot k \cdot \left(\sum_{j=1}^{j=m_1} F_j^d(t_p) \cdot \mathbf{E}_j^d \right) \cdot \left(\sum_{i=1}^{i=n} T_i(t_p) \cdot \mathbf{X}_i + \Upsilon(t_p) \cdot \mathbf{R} \right) \cdot \Delta t - \\ & - \mathbf{R}^T \cdot \left(\sum_{j=1}^{j=m_2} F_j^a(t_p) \cdot \mathbf{E}_j^a \right) \cdot \left(\sum_{l=1}^{l=L} C_l(t_p) \cdot \mathbf{D}_l \right) \cdot \Delta t = 0, \quad (67) \end{aligned}$$

that after making the indicated calculation results in a simple linear equation for each t_p :

$$\Upsilon(t_p) = a_p \cdot \Upsilon(t_{p-1}) + b_p, \quad \forall p \geq 1 \quad (68)$$

4. Numerical test

In this section we consider a numerical example consisting of a solid workpiece occupying at $t = 0$ the domain $\Omega^0 = (-0.5, 0.5) \times (0, 5)$. The piece is being compressed from its upper face. The domain evolves consequently to take intermediate configurations $\Omega(t)$ until reaching its final geometry at time $t = 1.28$. The tool of unit length $(-0.5, 0.5)$ is compressing the workpiece at a constant compression velocity. Assuming known the geometry evolution $\Omega(t)$

we are solving the thermal model defined in $\Omega(t)$ in a non-incremental way. We consider the following initial and boundary conditions:

$$\begin{cases} u(\mathbf{x} \in \Omega^0, t = 0) = 1 \\ u(\mathbf{x} \in \Gamma_c(t), t) = 0 \\ \nabla u(\mathbf{x} \in \Gamma_f(t), t) \cdot \mathbf{n} = 0 \end{cases} \quad (69)$$

where $\Gamma_c(t)$ and $\Gamma_f(t)$ represent the parts of the boundary of $\Omega(t)$, $\Gamma(t) \equiv \partial\Omega(t)$, in contact with the tool or the work plane $y = 0$ and the free boundary respectively.

After applying the strategy described in the previous section, $N = 15$ modes were found to be enough for representing the whole thermal history $u(\mathbf{x} \in \Omega(t), t)$:

$$\mathbf{U}^t \approx \sum_{i=1}^{i=15} T_i(t) \cdot \mathbf{X}_i \quad (70)$$

Functions T_i were computed only at times t_p and \mathbf{X}_i consists of a vector containing the nodal values related to any nodal distribution $\tilde{\mathbf{x}}_j^t$ in $\Omega(t)$.

For the sake of clarity we defined functions $G_i(t)$ by interpolating $T_i(t_p)$ values and defined functions $F_i(\mathbf{x} \in \Omega^0)$ by interpolating values in \mathbf{X}_i on the initial configuration Ω^0 . Fig 1 depicts the five most significant space modes F_i , $i = 1, \dots, 5$; as well as $G_i(t)$, $i = 1, \dots, 15$.

Now, we are in the position of assigning vectors \mathbf{X}_i to nodes $\tilde{\mathbf{x}}_j^t$ related to the configuration $\Omega(t)$ and then to reconstruct the solution in $\Omega(t)$. Figure 2 depicts the reconstructed temperature field in $\Omega(t)$ for six different time instants.

Figure 3 depicts, in turn, the error of the approximation for different number of terms in the approximation (ranging from 10 to 30) versus the incremental, standard, finite element solution of the problem.

5. Towards parametric modeling in evolving domains

The extension of the previously introduced technique to the case of parametric models on evolving domains is straightforward. To this end we should come back to section 3 and consider the parametric dependency of u on k , looking for the separated representation:

$$\mathbf{U}_k^t \approx \sum_{i=1}^{i=N} T_i(t) \cdot K_i(k) \cdot \mathbf{X}_i \quad (71)$$

For constructing such an approximation we proceed by computing a term of the finite sum at each iteration. Thus, we assume at iteration n that the n first terms of the sum have been already calculated, from which we can write the n -order approximation of \mathbf{U}_k^t

$$\mathbf{U}_k^t \approx \sum_{i=1}^{i=n} T_i(t) \cdot K_i(k) \cdot \mathbf{X}_i \quad (72)$$

Now, at the next iteration $n+1$ we look for the new functional product $T_{n+1}(t) \cdot K_{n+1} \cdot \mathbf{X}_{n+1}$. For the sake of simplicity functions $T_{n+1}(t)$, K_{n+1} and \mathbf{X}_{n+1} will be noted by Υ , W and \mathbf{R} respectively, where the dependence on t of Υ , and on k of W is omitted for the sake of clarity.

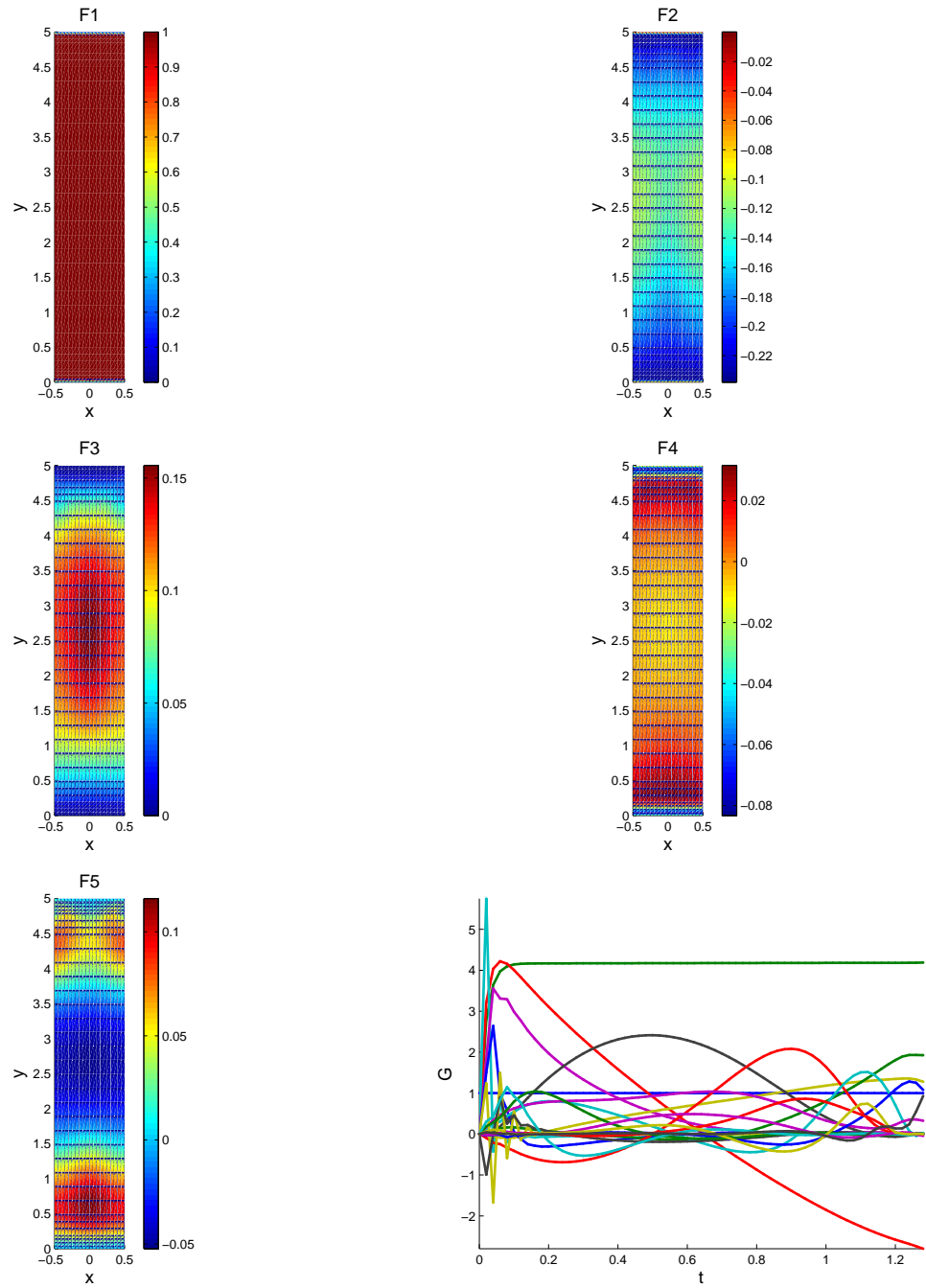


Figure 1. Space and time functions involved in the separated representation of $u(\mathbf{x} \in \Omega(t), t)$.

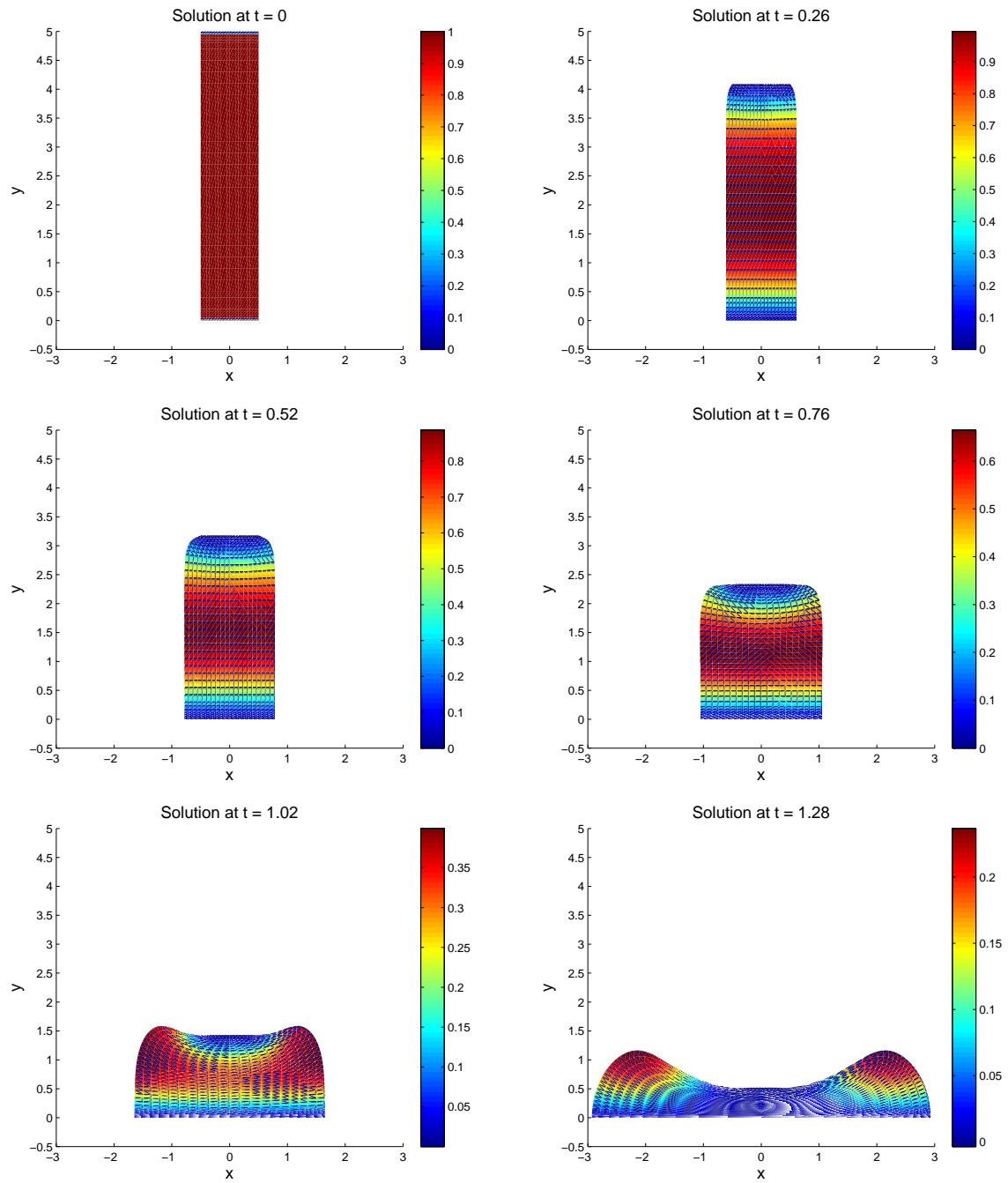


Figure 2. Reconstructed temperature field $u(\mathbf{x} \in \Omega(t), t)$ at six different instants.

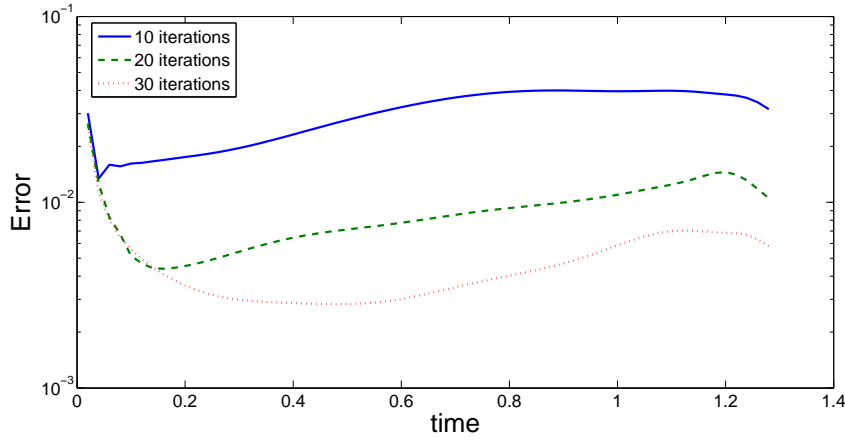


Figure 3. Error in the approximation for different number of terms in the sum. A standard, incremental finite element solution has been taken as reference.

Thus, the $(n + 1)$ -th order approximation reads:

$$\mathbf{U}_k^t \approx \sum_{i=1}^{i=n} T_i(t) \cdot K_i(k) \cdot \mathbf{X}_i + \Upsilon \cdot W \cdot \mathbf{R} \quad (73)$$

For computing functions Υ , W and \mathbf{R} we consider Eq. (58) where the trial function is given by (73) and the test function by:

$$\mathbf{U}^* = \Upsilon^* \cdot W \cdot \mathbf{R} + \Upsilon \cdot W^* \cdot \mathbf{R} + \Upsilon \cdot W \cdot \mathbf{R}^* \quad (74)$$

Since the resulting problem is non-linear because of the product of the three unknown functions Υ , W and \mathbf{R} a linearization is compulsory. The simplest one consists of the fixed point alternating directions strategy presented above. By generalizing the procedure widely described in section 3 we can compute the parametric and non-incremental separated representation. In the next section we consider the parametric solution of the problem solved in section 4.

6. Numerical test involving parametric modeling

In this section we consider the problem analyzed in section 4 where the material conductivity k is now considered as a model extra-coordinate taking values in the interval $k \in \mathfrak{S} = (0, 1)$. The strategy is now a mere combination of those applied for parametric problems in steady domains, and that for standard problems in evolving domains.

Fig 4 depicts the four most significant space modes F_i , $i = 1, \dots, 4$, where again F_i refers to the interpolation defined from values in \mathbf{X}_i on the initial configuration Ω^0 .

Fig. 5 depicts the most significant functions depending on time and on conductivity.

Finally, Fig. 6 depicts the temperature field reconstructed at the final geometry $\Omega(t = 1.28)$ for different values of the thermal conductivity. It can be noticed that the higher the conductivity the faster is the cooling process induced by the lower and constant temperatures enforced on the tool and working plane surfaces in contact with the workpiece.

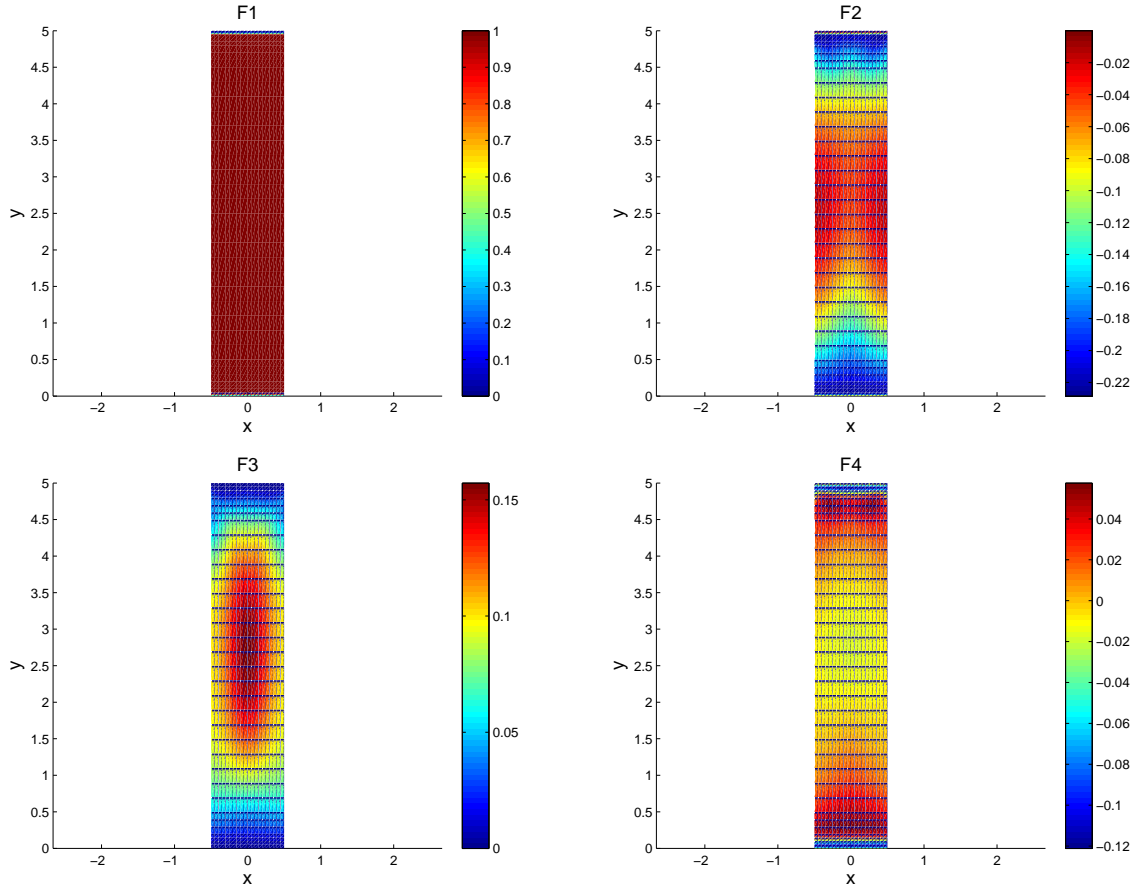


Figure 4. Four most significant space functions involved in the separated representation of $u(\mathbf{x} \in \Omega(t), t, k)$.

7. conclusions

In this paper a novel strategy for a priori construction of reduced bases for problems defined in evolving domains is presented. The main challenge in this class of problems derives precisely from the deformation of the problem domain, which prevents the direct application of classical, a posteriori, techniques such as proper orthogonal decomposition, to obtain appropriate reduced basis. The evolving nature of the domain obscures the concept of snapshot of the system state, requiring specific treatments.

However, it has been demonstrated that a combination of an updated Lagrangian approach for the description of domain's kinematics and a PGD-based obtention of the set of reduced basis in a separated space-time (possibly space-parameters-time) representation gives a very convenient way of constructing reduced basis. These basis can be advantageously employed to simulate complex problems at a very reduced CPU cost, as proven in the vast corps of

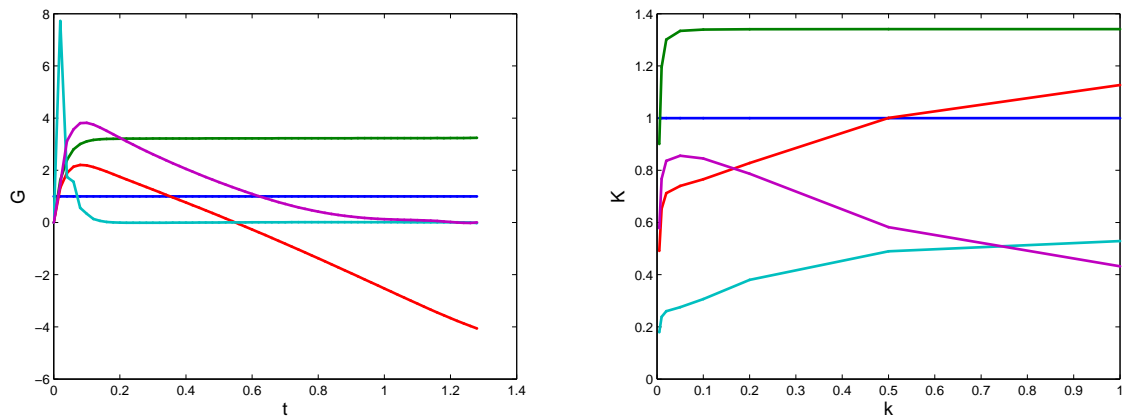


Figure 5. Most significant functions depending on the space and conductivity involved in the separated representation of $u(\mathbf{x} \in \Omega(t), t, k)$.

literature devoted to this end.

REFERENCES

1. I. Alfaro, J. Yvonnet, F. Chinesta, and E. Cueto. A study on the performance of Natural Neighbour-based Galerkin Methods. *International Journal for Numerical Methods in Engineering*, 71:1436–1465, 2007.
2. A. Ammar, F. Chinesta, P. Diez, and A. Huerta. An error estimator for separated representations of highly multidimensional models. *Computer Methods in Applied Mechanics and Engineering*, 199(25-28):1872 – 1880, 2010.
3. A. Ammar, B. Mokdad, F. Chinesta, and R. Keunings. A new family of solvers for some classes of multidimensional partial differential equations encountered in kinetic theory modeling of complex fluids. *J. Non-Newtonian Fluid Mech.*, 139:153–176, 2006.
4. A. Ammar, B. Mokdad, F. Chinesta, and R. Keunings. A new family of solvers for some classes of multidimensional partial differential equations encountered in kinetic theory modeling of complex fluids. part ii: transient simulation using space-time separated representations. *J. Non-Newtonian Fluid Mech.*, 144:98–121, 2007.
5. F. Chinesta, A. Ammar, and E. Cueto. Recent advances and new challenges in the use of the proper generalized decomposition for solving multidimensional models. *Archives of Computational Methods in Engineering*, 17:327–350, 2010.
6. F. Chinesta, P. Ladeveze, and E. Cueto. A short review on model order reduction based on proper generalized decomposition. *Archives of Computational Methods in Engineering*, 18:395–404, 2011.
7. E. Cueto, N. Sukumar, B. Calvo, M. A. Martínez, J. Cegonino, and M. Doblare. Overview and recent advances in Natural Neighbour Galerkin methods. *Archives of Computational Methods in Engineering*, 10(4):307–384, 2003.
8. J. Donea and A. Huerta. *Finite Element Methods for Flow Problems*. John Wiley and sons, 2003.
9. A. Falco and A. Nouy. Proper generalized decomposition for nonlinear convex problems in tensor banach spaces. *Numerische Mathematik*, pages 1–28. 10.1007/s00211-011-0437-5.
10. D. Gonzalez, A. Ammar, F. Chinesta, and E. Cueto. Recent advances on the use of separated representations. *International Journal of Numerical Methods in Engineering*, 85(5):637–659, 2010.
11. Ch. Heyberger, P.-A. Boucard, and D. Neron. Multiparametric analysis within the proper generalized decomposition framework. *Computational Mechanics*, 49:277–289, 2012. 10.1007/s00466-011-0646-x.
12. K. Karhunen. Über lineare methoden in der wahrscheinlichkeitsrechnung. *Ann. Acad. Sci. Fennicae, ser. Al. Math. Phys.*, 37, 1946.
13. P. Ladeveze. *Nonlinear Computational Structural Mechanics*. Springer, N.Y., 1999.

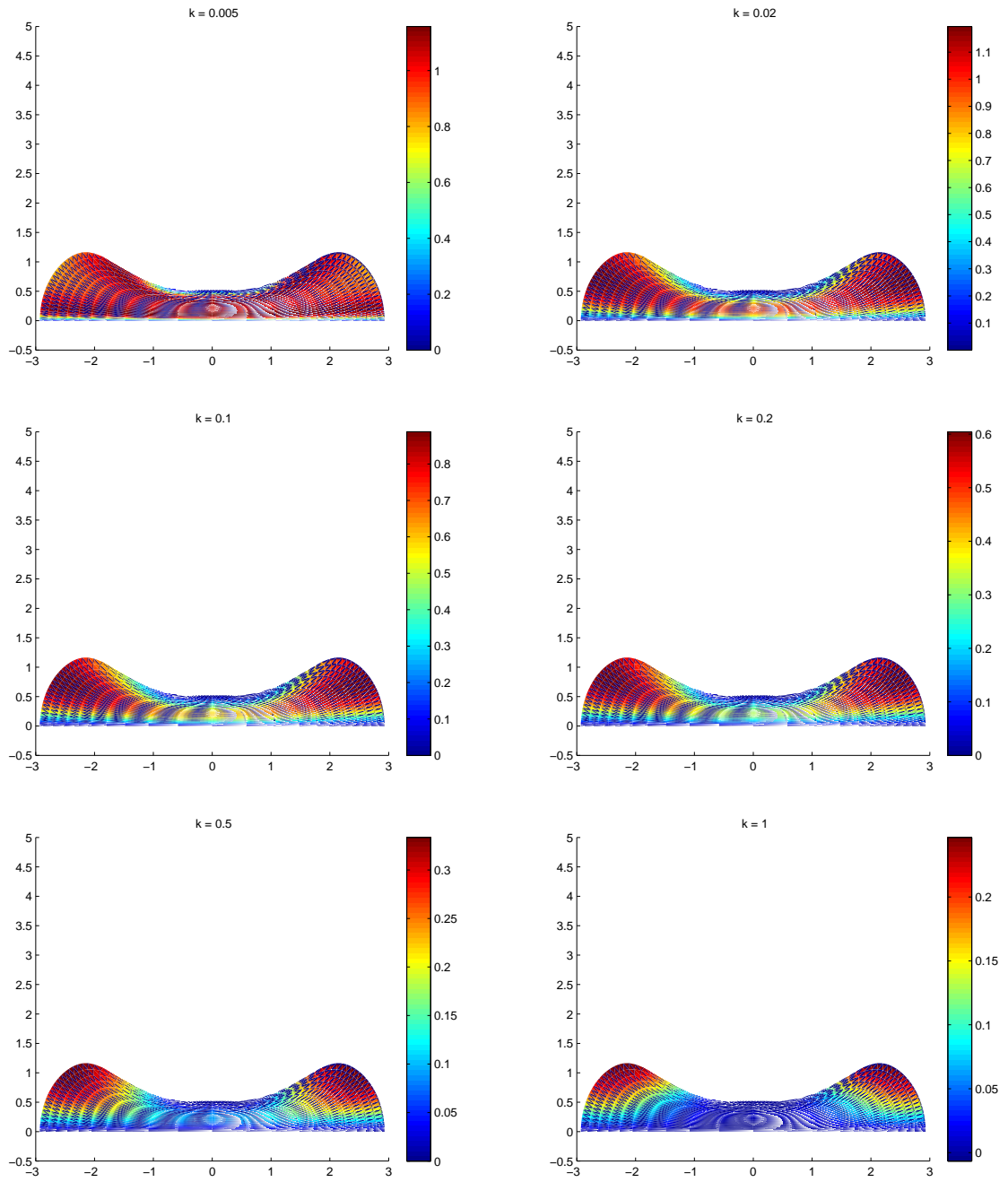


Figure 6. Reconstructed temperature field $u(\mathbf{x} \in \Omega(t = 1.28), t, k)$ for different values of the thermal conductivity k .

14. P. Ladeveze, J.C. Passieux, and D. Neron. The LATIN multiscale computational method and the Proper Generalized Decomposition. *COMPUTER METHODS IN APPLIED MECHANICS AND ENGINEERING*, 199(21-22, SI):1287–1296, 2010.
15. R. W. Lewis, S. E. Navti, and C. Taylor. A mixed lagrangian-eulerian approach to modelling fluid flow during mould filling. *International Journal for Numerical Methods in Fluids*, 25:931–952, 1997.
16. M. M. Loève. *Probability theory*. The University Series in Higher Mathematics, 3rd ed. Van Nostrand, Princeton, NJ, 1963.
17. E. N. Lorenz. *Empirical Orthogonal Functions and Statistical Weather Prediction*. MIT, Departement of Meteorology, Scientific Report Number 1, Statistical Forecasting Project, 1956.
18. A. Nouy. A priori model reduction through proper generalized decomposition for solving time-dependent partial differential equations. *Computer Methods in Applied Mechanics and Engineering*, 199(23-24):1603 – 1626, 2010.
19. E. Pruliere, F. Chinesta, and A. Ammar. On the deterministic solution of multidimensional parametric models using the Proper Generalized Decomposition. *MATHEMATICS AND COMPUTERS IN SIMULATION*, 81(4):791–810, DEC 2010.
20. D. Ryckelynck, F. Chinesta, E. Cueto, and A. Ammar. On the a priori Model Reduction: Overview and recent developments. *Archives of Computational Methods in Engineering*, 12(1):91–128, 2006.